

Magneto-thermo-elastic analysis of a functionally graded conical shell

A. Mehditabar, R. Akbari Alashti* and M.H. Pashaei

Mechanical Engineering Department, Babol University of Technology, Babol, Iran

(Received November 25, 2012, Revised September 05, 2013, Accepted September 18, 2013)

Abstract. In this paper, magneto-thermo-elastic problem of a thick truncated conical shell immersed in a uniform magnetic field and subjected to internal pressure is investigated. Material properties of the shell including the elastic modulus, magnetic permeability, coefficients of thermal expansion and conduction are assumed to be isotropic and graded through the thickness obeying the simple power law distribution, while the poisson's ratio is assumed to be constant. The temperature distribution is assumed to be a function of the thickness direction. Governing equations of the truncated conical shell are derived in terms of components of displacement and thermal fields and discretised with the help of differential quadrature (DQ) method. Results are obtained for different values of power law index of material properties and effects of thermal load on displacement, stress, temperature and magnetic fields are studied. Results of the present method are compared with those of the finite element method.

Keywords: Magneto-thermo-elastic; functionally graded material; truncated conical shell

1. Introduction

Truncated conical shells are well-known structural components which are extensively used in various branches of engineering applications such as pressure vessels, aerospace and ship building industries. In recent years, increased demands for mechanical components subjected to electro-magnetic, thermal and mechanical loadings have drawn the attention of researchers. Some of the common applications of interaction between these fields are found in geophysical studies, magnetically levitated vehicles, industrial heating equipments and cooking devices and other equipments working in combined magnetic and thermal environments.

On the other hand, a new class of advanced composite material called functionally graded material (FGM) is employed due to its improved thermal and mechanical characteristics. Material properties of FGMs vary gradually over the volume, by means of which features like high thermal load carrying capacity, wear and erosion resistant can be achieved.

Zhao and Liew (2011) carried out free vibration analysis of an FG conical shell panel using the element-free-kp-Ritz method. The first-order shear deformation shell theory and mesh-free kernel particle functions were employed to derive the fundamental relations. Sofiyev and Kuruoglu (2011) studied the nonlinear buckling behavior of cross ply laminated conical shells. The modified

*Corresponding author, Ph.D., E-mail: raalashti@nit.ac.ir

Donnell type stability and compatibility equations were obtained and solved analytically. Patel *et al.* (2005) carried out the investigation of thermo-elastic post-buckling behavior of cross-ply laminated composite conical shells under presumed uniform temperature distribution by employing semi-analytical finite element approach. Aghdam *et al.* (2011) investigated bending of moderately thick clamped FG conical panels subjected to uniform and non-uniform distributed loadings. The governing equations were derived using the first order shear deformation theory and solved with the help of Extended Kantorovich Method (EKM). Sofiyev (2012) studied the non-linear vibration of truncated conical shells made of FGM. Large deformation theory with von Karman-Donnell type of kinematic non-linearity was used for formulating the constitutive relations. Superposition, Galerkin and harmonic balance methods were applied to analyze problems.

Ying and Wang (2010) obtained an exact solution for two-dimensional analysis of finite hollow cylinder excited by non-uniform thermal shock. The solution was developed on the basis of uncoupled linear thermo-elastic theory, using the trigonometric series expansion method and the separation of variable technique. Shahani and Nabavi (2007) used the finite Hankel transform method to solve analytically the thermo-elasticity problem of a thick-walled cylinder. Chandrashekhara and Kumar (1993) have extended the solution to a thick, transversely isotropic, circular cylindrical shell subjected to axisymmetric loading. Also a transfer matrix approach has been presented to make the method computationally efficient. Eslami *et al.* (2005) obtained a general solution for the one-dimensional steady state thermal and mechanical stresses in a hollow thick sphere made of functionally graded material. The analytical solution of the heat conduction equation and the Navier equation was presented using the direct method. Sobhani Aragh and Yas (2010) presented three-dimensional analysis of thermal stresses in a four-parametric continuous grading fiber reinforced cylindrical panel subjected to thermal load. Generalized differential quadrature method was employed to solve the thermo-elastic equilibrium equations.

Khdeir (1996) investigated thermal deformations and stresses in a cross-ply laminated circular cylindrical shell. The state space approach was used to solve the thermo-elastic governing equations of the third-order and classical theories for arbitrary boundary conditions. Alibeigloo and Nouri (2010) presented three-dimensional solution for static analysis of functionally graded cylindrical shell with bonded piezoelectric layers using differential quadrature method. Dai *et al.* (2006, 2011) obtained an exact solution for the heat conduction problem of an FG hollow sphere using the direct method to solve the Navier equations. They also used infinitesimal theory to determine the exact solution of magneto-thermo-elastic behavior of functionally graded cylindrical and spherical vessels. Lee (2009) carried out three-dimensional axisymmetric magneto-thermo-elastic analysis for the laminated circular conical shells subjected to magnetic and vapor fields using Laplace and finite difference methods. Xing and Liu (2010) studied the behavior of magneto-thermo-elastic stresses in a conducting rectangular plate subjected to an arbitrary variation of magnetic field, employing the differential quadrature method.

Zielnica (2012) carried out buckling load and stability path analysis of a sandwich conical shell with unsymmetrical faces under combined loading condition based on the assumption of moderately large deflection. The constitutive relations were developed on the basis of the Nadai-Hencky deformation theory of plasticity and Prandtl-Reuss plastic flow theory and the Ritz method was used to solve the governing differential equations. Ghannad *et al.* (2012) performed an elastic analysis of axisymmetric clamped-clamped pressurized thick truncated conical shells made of functionally graded material, based on the first-order shear deformation theory. Matched asymptotic method (MAM) of the perturbation theory were used to convert the resulting equations

into a system of algebraic equations.

The main object of the present study is to investigate the magneto-thermo-elastic problem of a truncated conical shell made of functionally graded material subjected to a constant magnetic field, thermal load and internal pressure. Variations of material properties through the thickness of the shell are assumed to obey a simple power law. The fundamental equations of thermal and elastic fields are developed and an efficient semi-analytical method called differential quadrature (DQ) method is employed to approximate derivatives of functions along the thickness and the axial direction of generator. Results obtained by the present method are compared with those obtained by the finite element method which is found to be in excellent agreement. The effects of various parameters such as the power law index and thermal loading on the distribution of stress, displacement, temperature and induced magnetic field are graphically depicted.

2. Governing equations

Let us consider a truncated conical shell made of FGM with perfect conductivity permeated by initial magnetic field $H_{0\zeta}$ and subjected to uniform internal pressure P_0 and a rapid temperature change, T , at the inner surface. Physical model and corresponding system coordinates for the truncated conical shell is shown in Fig. 1., where h_{sh} denotes the thickness of the shell, L and L_1 are generatrix length and the distance between origin and top surface of cone, respectively and γ is the semi-vertex of the conical shell.

R_1 and R_2 indicate the inner radii of the cone at its small and large ends, respectively. The structure corresponds to coordinate system (s, θ, ζ) , where s lies along the generator and on the internal surface, θ axis lies in circumferential direction on the reference surface of the cone and the ζ axis is along the thickness direction of the cone.

The stiffness, magnetic permeability, coefficients of heat conductivity, thermal expansion and electric conductivity are assumed to vary through the wall thickness according to a simple power law distribution as follows

$$Y = Y_0 (1 + \zeta / h_{sh})^n \quad (1)$$

where Y_0 and n represent material properties at the inner surface and the power law index, respectively.

Let u and w be the displacement components in s and ζ directions, then the strain-displacement relations are given as

$$\begin{aligned} \varepsilon_{ss} &= \frac{\partial}{\partial s} u + 0.5 \left(\frac{\partial w}{\partial s} \right)^2 \\ \varepsilon_{\theta\theta} &= Z (w \cos(\gamma) + \sin(\gamma) u) + Z^2 (\cos(\gamma) \sin(\gamma) u w + 0.5 (\cos(\gamma)^2 w^2 + \sin(\gamma)^2 u^2)) \\ \varepsilon_{\zeta\zeta} &= \frac{\partial}{\partial \zeta} w + 0.5 \left(\frac{\partial w}{\partial s} \right)^2, \quad \varepsilon_{s\zeta} = \left(\frac{\partial u}{\partial \zeta} \right) + \left(\frac{\partial w}{\partial s} \right) + \left(\frac{\partial w}{\partial s} \right) \left(\frac{\partial w}{\partial \zeta} \right) \end{aligned} \quad (2)$$

where: $Z = \frac{1}{s \sin(\gamma) + \zeta \cos(\gamma)}$

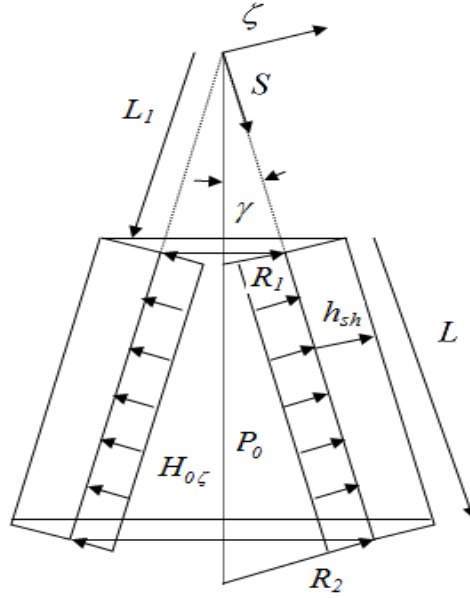


Fig. 1 Physical model and system coordinates for the truncated conical shell

The constitutive stress-strain relations for an isotropic material can be written in matrix form as

$$\begin{bmatrix} \sigma_{ss} \\ \sigma_{\theta\theta} \\ \sigma_{\zeta\zeta} \\ \tau_{s\zeta} \end{bmatrix} = \begin{bmatrix} c_{11} & c_{12} & c_{13} & 0 \\ c_{21} & c_{22} & c_{23} & 0 \\ c_{31} & c_{32} & c_{33} & 0 \\ 0 & 0 & 0 & c_{44} \end{bmatrix} \begin{bmatrix} \varepsilon_{ss} - \alpha T \\ \varepsilon_{\theta\theta} - \alpha T \\ \varepsilon_{\zeta\zeta} - \alpha T \\ \varepsilon_{s\zeta} \end{bmatrix} \quad (3)$$

where σ_{ij} and τ_{ij} represent the stresses and ε_{ij} represents the strain tensor and α is the coefficient of thermal expansion.

The quantities c_{ij} , $i, j = 1, 2, 3, 4$ for isotropic materials are defined by

$$\begin{aligned} c_{11} &= \lambda + 2G, & c_{12} &= \lambda, & c_{44} &= G, \\ c_{22} &= c_{33} = c_{11}, & c_{21} &= c_{13} = c_{31} = c_{12} = c_{23} = c_{32} \end{aligned} \quad (4)$$

where λ and G are Lamé's constants which are expressed as

$$\lambda = \frac{\nu E}{(1+\nu)(1-2\nu)}, \quad G = \frac{E}{2(1+\nu)} \quad (5)$$

By combining Eqs. (2) and (3), components of the stress field are defined in terms of components of the displacement and temperature fields.

$$\begin{aligned}
\sigma_{ss} &= c_{11} \left(\frac{\partial}{\partial s} u + 0.5 \left(\frac{\partial}{\partial s} w \right)^2 - \alpha T \right) \\
&\quad + c_{12} \left(Z(w \cos(\gamma) + \sin(\gamma)u) + Z^2 (\cos(\gamma) \sin(\gamma)uw) + 0.5 (\cos(\gamma)^2 w^2 + \sin(\gamma)^2 u^2) - \alpha T \right) \\
&\quad + c_{13} \left(\frac{\partial}{\partial \zeta} w + 0.5 \left(\frac{\partial}{\partial \zeta} w \right)^2 - \alpha T \right) \\
\sigma_{\theta\theta} &= c_{21} \left(\frac{\partial}{\partial s} u + 0.5 \left(\frac{\partial}{\partial s} w \right)^2 - \alpha T \right) \\
&\quad + c_{22} \left(Z(w \cos(\gamma) + \sin(\gamma)u) + Z^2 (\cos(\gamma) \sin(\gamma)uw + 0.5 (\cos(\gamma)^2 w^2 + \sin(\gamma)^2 u^2)) - \alpha T \right) \\
&\quad + c_{23} \left(\frac{\partial}{\partial \zeta} w + 0.5 \left(\frac{\partial}{\partial \zeta} w \right)^2 - \alpha T \right) \\
\sigma_{\zeta\zeta} &= c_{31} \left(\frac{\partial}{\partial s} u + 0.5 \left(\frac{\partial}{\partial s} w \right)^2 - \alpha T \right) \\
&\quad + c_{32} \left(Z(w \cos(\gamma) + \sin(\gamma)u) + Z^2 (\cos(\gamma) \sin(\gamma)uw + 0.5 (\cos(\gamma)^2 w^2 + \sin(\gamma)^2 u^2)) - \alpha T \right) \\
&\quad + c_{23} \left(\frac{\partial}{\partial \zeta} w + 0.5 \left(\frac{\partial}{\partial \zeta} w \right)^2 - \alpha T \right) \\
\tau_{s\zeta} &= c_{44} \left(\left(\frac{\partial}{\partial \zeta} u \right) + \left(\frac{\partial}{\partial s} w \right) + \left(\frac{\partial}{\partial s} w \right) \left(\frac{\partial}{\partial \zeta} w \right) \right)
\end{aligned} \tag{6}$$

Assuming that the magnetic field vector in the conducting truncated conical shell, has only one component that acts along the thickness $\vec{H} = (0, 0, H_{0\zeta})$, then by disregarding the displacement current, the governing equations and fundamental relations of electro-dynamic Maxwell equations (John 1941) for a perfectly conducting, elastic-body is presented as

$$\vec{h} = \text{curl}(\vec{U} \times \vec{H}), \quad \text{div} h = 0, \quad \vec{J} = \nabla \times \vec{h} \tag{7}$$

where \vec{J} , \vec{h} and \vec{U} represent electric current density, induced magnetic field and displacement vectors, respectively.

In order to obtain the induced magnetic field vector \vec{h} from Eq. (7), we have to invoke the following relation (Strang 1986)

$$\text{curl}(\vec{U} \times \vec{H}) = U \text{div}(\vec{H}) - \vec{H} \text{div}(\vec{U}) + (\vec{H} \cdot \nabla) \vec{U} - (\vec{U} \cdot \nabla) \vec{H} \tag{8}$$

It is observed from Eqs. (7) and (8) that a key problem to obtain the induced magnetic field vector, is to have the divergence and curl of the vector function $X (v_s, v_\theta, v_\zeta)$, in the conical coordinate system (s, θ, ζ) , which are defined by the following formulas

$$\begin{aligned}
\text{div}(v) &= \frac{\partial v_s}{\partial s} + \frac{\partial v_\zeta}{\partial \zeta} + Z \left(\frac{\partial v_\theta}{\partial \theta} + v_s \sin(\gamma) + v_\zeta \cos(\gamma) \right) \\
\text{curl}(v) &= \left(Z \left(\frac{\partial v_\zeta}{\partial \theta} - \frac{\partial}{\partial \zeta} (Z v_\theta) \right) \right), \quad \frac{\partial v_\zeta}{\partial \theta} - \frac{\partial}{\partial \zeta}, \quad Z \left(\frac{\partial}{\partial s} (Z v_\theta) - \frac{\partial v_s}{\partial \theta} \right)
\end{aligned} \tag{9}$$

By substituting magnetic field vector \vec{H} and displacement vector \vec{U} in Eq. (7) and employing Eq. (8), the induced magnetic field vector \vec{h} is obtained which has two components in the s and ζ directions. The current density vector \vec{J} , is found to have one component in the θ -direction as follow

$$\begin{aligned}
\vec{h} &= (h_s, h_\theta, h_\zeta), \\
h_s &= \left(\frac{\partial u}{\partial \zeta} + Z \cos(\gamma) u \right) H_{0\zeta}, \quad h_\zeta = - \left(\frac{\partial u}{\partial s} + Z \sin(\gamma) u \right) H_{0\zeta} \\
\vec{J} &= (J_s, J_\theta, J_\zeta), \\
J_\theta &= \left(\frac{\partial^2 u}{\partial s^2} + \frac{\partial^2 u}{\partial \zeta^2} + Z \left(\sin(\gamma) \left(\frac{\partial u}{\partial s} - Z \sin(\gamma) u \right) + \cos(\gamma) \left(\frac{\partial u}{\partial \zeta} - Z \cos(\gamma) u \right) \right) \right) H_{0\zeta}
\end{aligned} \tag{10}$$

The conducting truncated conical shell immersed in a magnetic field, $H_{0\zeta}$, is subjected to Lorentz's force. Lorentz's force vector has only one nonzero component which is along the s direction, as follow

$$\begin{aligned}
f_i &= \mu(\zeta) (\vec{J} \times \vec{H}), \quad f_i = (f_s, f_\theta, f_\zeta), \quad f_\theta = 0, \quad f_\zeta = 0 \\
f_s &= \mu_0 (1 + \zeta / h_{sh})^n H_{0\zeta}^2 \left(\frac{\partial^2 u}{\partial s^2} + \frac{\partial^2 u}{\partial \zeta^2} + Z \left(\sin(\gamma) \left(\frac{\partial u}{\partial s} - Z \sin(\gamma) u \right) + \cos(\gamma) \left(\frac{\partial u}{\partial \zeta} - Z \cos(\gamma) u \right) \right) \right)
\end{aligned} \tag{11}$$

The two-dimensional equilibrium equations in s and ζ directions taking to account of the Lorentz's force f_i , are expressed as

$$\begin{aligned}
\frac{\partial}{\partial s} \sigma_{ss} + \frac{\partial}{\partial \zeta} \tau_{s\zeta} + Z \left((\sigma_{ss} - \sigma_{\theta\theta}) \sin(\gamma) + \tau_{s\zeta} \cos(\gamma) \right) + f_s &= 0 \\
\frac{\partial}{\partial s} \tau_{s\zeta} + \frac{\partial}{\partial \zeta} \sigma_{\zeta\zeta} + Z \left(\tau_{s\zeta} \sin(\gamma) + (\sigma_{\zeta\zeta} - \sigma_{\theta\theta}) \cos(\gamma) \right) + f_\zeta &= 0
\end{aligned} \tag{12}$$

By substituting Eqs. (6) and (11) into Eq. (12), equilibrium equations in s and ζ directions are obtained in terms of components of the displacement and temperature fields in Eqs. (13a) and (13b), respectively as follows

$$\begin{aligned}
 & \left. \begin{aligned}
 & \frac{\partial}{\partial s} \left(\frac{E_0(1+\zeta/h_{sh})^n}{(1+\nu)(1-2\nu)} (1-\nu) \left(\frac{\partial}{\partial s} u + 0.5 \left(\frac{\partial}{\partial s} w \right)^2 \right) \right) \\
 & + \nu \left(\frac{\partial}{\partial \zeta} \left(Z^2 (\cos(\gamma) \sin(\gamma) uw) + 0.5 (\cos(\gamma)^2 w^2 + \sin(\gamma)^2 u^2) \right) \right. \\
 & \left. + Z (w \cos(\gamma) \sin(\gamma)) + \frac{\partial}{\partial \zeta} w + 0.5 \left(\frac{\partial}{\partial \zeta} w \right)^2 \right) - \alpha_0 \left(1 + \frac{\zeta}{h_{sh}} \right)^n T \\
 & + \frac{\partial}{\partial \zeta} \left(\frac{E_0(1+\zeta/h_{sh})^n}{2(1+\nu)} \left(\left(\frac{\partial}{\partial \zeta} u \right) + \left(\frac{\partial}{\partial s} w \right) + \left(\frac{\partial}{\partial s} w \right) \left(\frac{\partial}{\partial \zeta} w \right) \right) \right) \\
 & + Z \left(\frac{E_0(1+\zeta/h_{sh})^n}{(1+\nu)} \sin(\gamma) \left(\frac{\partial}{\partial \zeta} u + 0.5 \left(\frac{\partial}{\partial s} w \right)^2 - \left(Z^2 (\cos(\gamma) \sin(\gamma) uw) \right. \right. \right. \\
 & \left. \left. \left. + 0.5 (\cos(\gamma)^2 w^2 + \sin(\gamma)^2 u^2) \right) \right) \right) \right) \\
 & + \frac{E_0(1+\zeta/h_{sh})^n}{2(1+\nu)} \cos(\gamma) \left(\left(\frac{\partial}{\partial \zeta} u \right) + \left(\frac{\partial}{\partial s} w \right) + \left(\frac{\partial}{\partial s} w \right) \left(\frac{\partial}{\partial \zeta} w \right) \right) \\
 & + \mu_0 (1+\zeta/h_{sh})^n H_{0\zeta}^2 \left(\frac{\partial^2 u}{\partial s^2} + \frac{\partial^2 u}{\partial \zeta^2} + Z \sin(\gamma) \left(\frac{\partial u}{\partial s} - Z \sin(\gamma) u \right) \right. \\
 & \left. + Z \cos(\gamma) \left(\frac{\partial u}{\partial s} - Z \cos(\gamma) u \right) \right) = 0
 \end{aligned} \right) \quad (13a)
 \end{aligned}$$

$$\begin{aligned}
 & \frac{\partial}{\partial s} \left(\frac{E_0(1+\zeta/h_{sh})^n}{2(1+\nu)} \left(\left(\frac{\partial}{\partial \zeta} u \right) + \left(\frac{\partial}{\partial s} w \right) + \left(\frac{\partial}{\partial s} w \right) \left(\frac{\partial}{\partial \zeta} w \right) \right) \right) \\
 & + \frac{\partial}{\partial \zeta} \left(\frac{E_0(1+\zeta/h_{sh})^n}{(1+\nu)(1-2\nu)} \left(\nu \left(\frac{\partial}{\partial s} u + 0.5 \left(\frac{\partial}{\partial s} w \right)^2 + Z (w \cos(\gamma) + u \sin(\gamma)) \right) \right. \right. \\
 & \left. \left. + Z^2 \left(\cos(\gamma) \sin(\gamma) uw + 0.5 (\cos(\gamma)^2 w^2 + \sin(\gamma)^2 u^2) \right) \right) \right. \\
 & \left. + (1-\nu) \left(\left(\frac{\partial}{\partial \zeta} w \right) + 0.5 \left(\frac{\partial}{\partial \zeta} w \right)^2 \right) - \alpha_0 \left(1 + \frac{\zeta}{h_{sh}} \right)^n T \right) \\
 & + Z \left(\frac{E_0(1+\zeta/h_{sh})^n}{2(1+\nu)} \sin(\gamma) \left(\left(\frac{\partial}{\partial \zeta} u \right) + \left(\frac{\partial}{\partial s} w \right) + \left(\frac{\partial}{\partial s} w \right) \left(\frac{\partial}{\partial \zeta} w \right) \right) \right. \\
 & \left. - \frac{E_0(1+\zeta/h_{sh})^n}{(1+\nu)} \cos(\gamma) \left(Z (w \cos(\gamma) + u \sin(\gamma)) + Z^2 \left(\cos(\gamma) \sin(\gamma) uw \right. \right. \right. \\
 & \left. \left. \left. + 0.5 (\cos(\gamma)^2 w^2 + \sin(\gamma)^2 u^2) \right) \right) \right. \\
 & \left. - \left(\left(\frac{\partial}{\partial \zeta} w \right) + 0.5 \left(\frac{\partial}{\partial \zeta} w \right)^2 \right) \right) = 0 \quad (13b)
 \end{aligned}$$

In this study, the inner surface of the truncated conical shell is subjected to boundary temperature T , uniform pressure P_0 and initial magnetic field $H_{0\zeta}$. It is also supposed that the outer radius is free of traction and its temperature is kept at 0° . Considering these details, the mechanical, thermal and magnetic boundary conditions at the inner and outer boundary surfaces are described as

$$\begin{aligned} \zeta = 0, \quad \sigma_{\zeta\zeta} = P_0, \quad \tau_{s\zeta} = 0, \quad T_i = T, \quad H = H_{0\zeta}, \\ \zeta = h_{sh}, \quad \sigma_{\zeta\zeta} = 0, \quad \tau_{s\zeta} = 0, \quad T_0 = T, \quad H = 0 \end{aligned} \quad (14)$$

It is also assumed that the top and bottom boundaries of the cone are clamped, thus these boundary conditions are expressed as

$$\begin{aligned} s = L_1, \quad u = 0, \quad w = 0, \\ s = L_1 + L, \quad u = 0, \quad w = 0 \end{aligned} \quad (15)$$

The heat conduction equation in the steady-state condition for the truncated conical shell can be written as

$$\left(\frac{K \cos(\gamma)}{R_1 + 1/A} \right) \frac{\partial}{\partial \zeta} T + K \frac{\partial^2 T}{\partial \zeta^2} + \frac{\partial}{\partial \zeta} K \frac{\partial}{\partial \zeta} T = 0 \quad (16)$$

where K is the coefficient of heat conductivity.

3. Method of solution

The differential quadrature technique is applied as a semi-analytical procedure to discretize governing and related boundary equations. Differential quadrature method approximates the derivatives of a smooth function by a linear summation of all the functional values along an assumed mesh line. In this investigation, weighting coefficients related to the first-order derivative are obtained based on the Lagrange interpolation. For higher order derivatives the matrix multitude approach is used (Shu 2000).

$$A_{i,j}^{(1)} = \frac{1}{x_j - x_i} \prod_{\substack{k=1 \\ k \neq i,j}}^N \frac{x_i - x_k}{x_j - x_k}, \quad i \neq j, \quad A_{i,j}^{(1)} = \prod_{\substack{k=1 \\ k \neq i,j}}^N \frac{1}{x_j - x_k}, \quad A_{i,j}^{(2)} = \sum_{k=1}^N A_{i,k}^{(1)} A_{k,j}^{(1)} \quad (17)$$

where $A^{(n)}$ shows the weighting coefficients for the n^{th} order derivative.

Above formulation belongs to one-dimensional problem. The first and the second order derivatives of the goal function are developed by extending one-dimensional differential quadrature approximations to a two-dimensional case which can be described by

$$\begin{aligned} \frac{\partial f}{\partial \zeta} = \sum_{k=1}^N A_{i,n}^{(1)} f_{n,j}, \quad \frac{\partial^2 f}{\partial \zeta^2} = \sum_{k=1}^N A_{i,n}^{(2)} f_{n,j}, \quad \frac{\partial f}{\partial s} = \sum_{l=1}^P B_{j,l}^{(1)} f_{i,l}, \quad \frac{\partial^2 f}{\partial s^2} = \sum_{l=1}^P B_{i,l}^{(2)} f_{i,l} \\ \frac{\partial^2 f}{\partial s \partial \zeta} = \sum_{n=1}^N \sum_{l=1}^P A_{i,n}^{(1)} B_{j,l}^{(1)} f_{i,j} \end{aligned} \quad (18)$$

where $A^{(n)}$, $B^{(n)}$ represent weighting coefficients for the n^{th} derivative along the thickness and generator directions; P and N are the numbers of sampling points along the generatrix direction s and thickness direction ζ , respectively. Transversely discretized governing differential equations and the related boundary conditions are transformed into algebraic equations using DQ method. The quadrature form of equilibrium equations i.e., Eqs. (13a) and (13b) are substituted in Eqs. (19a) and (19b), respectively.

$$\frac{E(1 + \zeta_i / h_{sh})^n}{(1 + \nu)(1 - 2\nu)} \left(\begin{aligned} & (1 - \nu) \left(\sum_{l=1}^P B_{j,l}^{(2)} u_{i,l} \right) \\ & + \left(\sum_{l=1}^P B_{j,l}^{(1)} w_{i,l} \right) \left(\sum_{l=1}^P B_{j,l}^{(2)} w_{i,l} \right) \\ & + \nu \left(-2 \sin(\gamma) Z^3 \cos(\gamma) \sin(\gamma) u_{i,k} w_{i,k} \right) \\ & + 0.5 \left(\cos(\gamma)^2 w_{i,k}^2 + \sin(\gamma)^2 u_{i,k}^2 \right) \\ & + Z^2 \left(\cos(\gamma) \sin(\gamma) \left(\sum_{l=1}^P B_{j,l}^{(1)} u_{i,l} \right) w_{i,k} + \left(\sum_{l=1}^P B_{j,l}^{(1)} w_{i,l} \right) u_{i,k} \right) \\ & + \cos(\gamma)^2 \left(\sum_{l=1}^P B_{j,l}^{(1)} w_{i,l} \right) w_{i,j,k} + \sin(\gamma)^2 \left(\sum_{l=1}^P B_{j,l}^{(1)} u_{i,l} \right) u_{i,k} \\ & - \sin(\gamma) Z^2 \left(w_{i,k} \cos(\gamma) + u_{i,k} \sin(\gamma) \right) + Z \left(\sum_{l=1}^P B_{j,l}^{(1)} w_{i,l} \right) \cos(\gamma) \\ & + \left(\sum_{l=1}^P B_{j,l}^{(1)} u_{i,l} \right) \sin(\gamma) \\ & + \sum_{n=1}^N \sum_{l=1}^P A_{i,n}^{(1)} B_{j,l}^{(1)} w_{i,j} + \left(\sum_{n=1}^N A_{i,n}^{(1)} w_{i,j} \right) \left(\sum_{n=1}^N \sum_{l=1}^P A_{i,n}^{(1)} B_{j,l}^{(1)} w_{i,j} \right) \end{aligned} \right) \quad (19a)$$

$$+ \frac{E \frac{n}{h_{sh}} (1 + \zeta_i / h_{sh})^{n-1}}{2(1 + \nu)} \left(\left(\sum_{n=1}^N A_{i,n}^{(1)} u_{n,j} \right) + \left(\sum_{l=1}^P B_{j,l}^{(1)} w_{i,j} \right) + \left(\sum_{l=1}^P B_{j,l}^{(1)} w_{i,l} \right) \left(\sum_{n=1}^N A_{i,n}^{(1)} w_{n,j} \right) \right)$$

$$+ \frac{E(1 + \zeta_i / h_{sh})^n}{2(1 + \nu)} \left(\begin{aligned} & \left(\sum_{n=1}^N A_{i,n}^{(2)} u_{n,j} \right) + \left(\sum_{n=1}^N \sum_{l=1}^P A_{i,n}^{(1)} B_{j,l}^{(1)} w_{i,j} \right) \\ & + \left(\sum_{n=1}^N \sum_{l=1}^P A_{i,n}^{(1)} B_{j,l}^{(1)} w_{i,j} \right) \left(\sum_{n=1}^N A_{i,n}^{(1)} w_{n,j} \right) \\ & + \left(\sum_{l=1}^P B_{j,l}^{(1)} w_{i,l} \right) \left(\sum_{n=1}^N A_{i,n}^{(2)} w_{n,j} \right) \end{aligned} \right)$$

$$\begin{aligned}
& + Z \left(\begin{aligned} & \sin(\gamma) \frac{E(1 + \zeta_i / h_{sh})^n}{(1 + \nu)} \left(\begin{aligned} & \sum_{l=1}^P B_{j,l}^{(1)} u_{i,l} + 0.5 \left(\sum_{l=1}^P B_{j,l}^{(1)} w_{i,l} \right)^2 \\ & - \left(Z^2 \left(\begin{aligned} & \cos(\gamma) \sin(\gamma) u_{i,k} w_{i,k} \\ & + 0.5 (\cos(\gamma)^2 w_{i,k}^2 + \sin(\gamma)^2 u_{i,k}^2) \end{aligned} \right) \right. \\ & \left. + Z (w_{i,k} \cos(\gamma) + u_{i,k} \sin(\gamma)) \right) \end{aligned} \right) \\ & + \frac{E(1 + \zeta_i / h_{sh})^n}{2(1 + \nu)} \cos(\gamma) \left(\begin{aligned} & \left(\sum_{n=1}^N A_{i,n}^{(1)} u_{n,j} \right) + \left(\sum_{l=1}^P B_{j,l}^{(1)} w_{i,l} \right) \\ & + \left(\sum_{l=1}^P B_{j,l}^{(1)} w_{i,l} \right) \left(\sum_{n=1}^N A_{i,n}^{(1)} w_{n,j} \right) \end{aligned} \right) \end{aligned} \right) \quad (19a) \\
& + \mu_0 E(1 + \zeta_i / h_{sh})^n H_{0\zeta}^2 \left(\begin{aligned} & \sum_{l=1}^P B_{j,l}^{(2)} u_{i,l} + Z \sin(\gamma) \left(\left(\sum_{l=1}^P B_{j,l}^{(1)} u_{i,l} \right) - Z u_{i,k} \sin(\gamma) \right) \\ & + \sum_{n=1}^N A_{i,n}^{(2)} u_{n,j} + Z \cos(\gamma) \left(\left(\sum_{n=1}^N A_{i,n}^{(1)} u_{n,j} \right) - Z u_{i,k} \cos(\gamma) \right) \end{aligned} \right) = 0
\end{aligned}$$

$$\frac{E(1 + \zeta_i / h_{sh})^n}{2(1 + \nu)} \left(\begin{aligned} & \left(\sum_{n=1}^N \sum_{l=1}^P A_{i,n}^{(1)} B_{j,l}^{(1)} u_{i,j} \right) + \left(\sum_{l=1}^P B_{j,l}^{(2)} w_{i,l} \right) + \left(\sum_{l=1}^P B_{j,l}^{(2)} w_{i,l} \right) \left(\sum_{n=1}^N A_{i,n}^{(1)} w_{n,j} \right) \\ & + \left(\sum_{l=1}^P B_{j,l}^{(1)} w_{i,l} \right) \left(\sum_{n=1}^N \sum_{l=1}^P A_{i,n}^{(1)} B_{j,l}^{(1)} w_{i,j} \right) \end{aligned} \right)$$

$$\begin{aligned}
& + \frac{n}{h_{sh}} \frac{E(1 + \zeta_i / h_{sh})^{n-1}}{(1 + \nu)(1 - 2\nu)} \left(\begin{aligned} & \left(\begin{aligned} & \sum_{l=1}^P B_{j,l}^{(1)} u_{i,l} + 0.5 \left(\sum_{l=1}^P B_{j,l}^{(1)} w_{i,l} \right)^2 \\ & + Z^2 \left(\begin{aligned} & \cos(\gamma) \sin(\gamma) u_{i,k} w_{i,k} \\ & 0.5 (\cos(\gamma)^2 w_{i,k}^2 + \sin(\gamma)^2 u_{i,k}^2) \end{aligned} \right) \\ & + Z (w_{i,j,k} \cos(\gamma) + u_{i,k} \sin(\gamma)) \end{aligned} \right) \\ & + (1 - \nu) \left(\begin{aligned} & \sum_{n=1}^N A_{i,n}^{(1)} w_{i,j} \\ & + 0.5 \left(\sum_{n=1}^N A_{i,n}^{(1)} w_{n,j} \right)^2 \end{aligned} \right) - \alpha_0 \left(1 + \frac{\zeta_i}{h_{sh}} \right)^n T_{i,k} \end{aligned} \right) \quad (19b)
\end{aligned}$$

$$\begin{aligned}
 & \left(\begin{aligned}
 & \sum_{n=1}^N \sum_{l=1}^P A_{i,n}^{(1)} B_{j,l}^{(1)} u_{i,j} + \left(\sum_{l=1}^P B_{j,l}^{(1)} w_{i,l} \right) \left(\sum_{n=1}^N \sum_{l=1}^P A_{i,n}^{(1)} B_{j,l}^{(1)} w_{i,j} \right) \\
 & + Z^2 \left(\cos(\gamma) \sin(\gamma) \left(\sum_{n=1}^N A_{i,n}^{(1)} u_{n,j} \right) w_{i,k} + \left(\sum_{n=1}^N A_{i,n}^{(1)} w_{n,j} \right) u_{i,k} \right) \\
 & \left. + \cos(\gamma)^2 w_{i,k} \left(\sum_{n=1}^N A_{i,n}^{(1)} w_{n,j} \right) + \sin(\gamma)^2 u_{i,k} \left(\sum_{n=1}^N A_{i,n}^{(1)} u_{n,j} \right) \right) \\
 & - 2 \cos(\gamma) Z^3 \left(\cos(\gamma) \sin(\gamma) u_{i,k} w_{i,k} \right. \\
 & \left. + 0.5 \left(\cos(\gamma)^2 w_{i,k}^2 + \sin(\gamma)^2 u_{i,k}^2 \right) \right) \\
 & + Z \left(\left(\sum_{n=1}^N A_{i,n}^{(1)} w_{n,j} \right) \cos(\gamma) \right) - \cos(\gamma) Z^2 \left(\begin{aligned}
 & w_{i,k} \cos(\gamma) \\
 & + u_{i,k} \sin(\gamma)
 \end{aligned} \right) \\
 & \left. + \left(\sum_{n=1}^N A_{i,n}^{(1)} u_{n,j} \right) \sin(\gamma) \right) \\
 & + (1-\nu) \left(\sum_{n=1}^N A_{i,n}^{(2)} w_{n,j} + \left(\sum_{n=1}^N A_{i,n}^{(2)} w_{n,j} \right) \left(\sum_{n=1}^N A_{i,n}^{(1)} w_{n,j} \right) \right) \\
 & - \alpha_0 \left(1 + \frac{\zeta_i}{h_{sh}} \right)^n \left(\sum_{n=1}^N A_{i,n}^{(1)} T_{n,j} \right) \\
 & - \alpha_0 \frac{n}{h_{sh}} \left(1 + \frac{\zeta_i}{h_{sh}} \right)^{n-1} T_{i,k}
 \end{aligned} \right) \tag{19b}
 \end{aligned}$$

$$\begin{aligned}
 & \left(\begin{aligned}
 & \frac{E(1 + \zeta_i / h_{sh})^n}{2(1 + \nu)} \sin(\gamma) \left(\left(\sum_{n=1}^N A_{i,n}^{(1)} u_{n,j} \right) + \left(\sum_{l=1}^P B_{j,l}^{(1)} w_{i,l} \right) \right) \\
 & + \left(\sum_{l=1}^P B_{j,l}^{(1)} w_{i,l} \right) \left(\sum_{n=1}^N A_{i,n}^{(1)} w_{n,j} \right) \\
 & Z \left(\begin{aligned}
 & w_{i,k} \cos(\gamma) \\
 & + u_{i,k} \sin(\gamma)
 \end{aligned} \right) \\
 & - \frac{E(1 + \zeta_i / h_{sh})^n}{2(1 + \nu)} \cos(\gamma) \left(\begin{aligned}
 & \cos(\gamma) \sin(\gamma) u_{i,k} w_{i,k} \\
 & + Z^2 \left(\begin{aligned}
 & \cos(\gamma)^2 w_{i,k}^2 \\
 & + \sin(\gamma)^2 u_{i,k}^2
 \end{aligned} \right) \\
 & - \left(\sum_{n=1}^N A_{i,n}^{(1)} w_{n,j} + 0.5 \left(\sum_{n=1}^N A_{i,n}^{(1)} w_{n,j} \right)^2 \right)
 \end{aligned} \right) \right) = 0
 \end{aligned} \right)
 \end{aligned}$$

And the corresponding mechanical boundary conditions are transformed into the following form

$$\sigma_{\zeta\zeta} = \frac{E_0(1 + \zeta_i / h_{sh})^n}{(1 + \nu)(1 - 2\nu)} \left(\begin{array}{l} \left(\sum_{l=1}^P B_{j,l}^{(1)} u_{i,l} + 0.5 \left(\sum_{l=1}^P B_{j,l}^{(1)} u_{i,l} \right)^2 \right) \\ \nu + Z^2 \left(\begin{array}{l} \cos(\gamma) \sin(\gamma) u_{i,k} w_{i,k} \\ + \frac{1}{2} (\cos(\gamma)^2 w_{i,k}^2 + \sin(\gamma)^2 u_{i,k}^2) \end{array} \right) \\ + Z \left(\begin{array}{l} w_{i,k} \cos(\gamma) \\ + u_{i,k} \sin(\gamma) \end{array} \right) \end{array} \right) = 0 \quad (20a)$$

$$+ (1 - \nu) \left(\begin{array}{l} \sum_{n=1}^N A_{i,n}^{(1)} w_{n,j} \\ + 0.5 \left(\sum_{n=1}^N A_{i,n}^{(1)} w_{n,j} \right)^2 \end{array} \right) - \alpha_0 (1 + \zeta_i / h_{sh})^n T_{i,k}$$

$$\sigma_{s\zeta} = \frac{E_0(1 + \zeta_i / h_{sh})^n}{2(1 + \nu)} \left(\begin{array}{l} \left(\sum_{n=1}^N A_{i,n}^{(1)} u_{n,j} + \left(\sum_{l=1}^P B_{j,l}^{(1)} w_{i,l} \right) \right) \\ + \left(\sum_{l=1}^P B_{j,l}^{(1)} w_{i,l} \right) \left(\sum_{n=1}^N A_{i,n}^{(1)} w_{n,j} \right) \end{array} \right) = 0 \quad (20b)$$

And the discretised heat conduction equation is obtained as follows

$$\left(\frac{K_0(1 + \zeta_i / h_{sh})^n \cos(\gamma)}{R_1 + 1/Z} \right) \left(\sum_{n=1}^N A_{i,n}^{(1)} T_{n,j} \right) + K_0(1 + \zeta_i / h_{sh})^n \left(\sum_{n=1}^N A_{i,n}^{(2)} T_{n,j} \right) + K_0 \frac{n}{h} (1 + \zeta_i / h_{sh})^{n-1} \left(\sum_{n=1}^N A_{i,n}^{(1)} T_{n,j} \right) = 0 \quad (21)$$

4. Numerical results and discussion

In numerical calculations, geometrical parameters of $L = 1$, $\gamma = 15^\circ$ for the truncated conical shell are assumed. Sampling points with following coordinate can be obtained using the Chebyshev-Gauss-Lobatto formula as follow:

In the s - direction

$$s_i = L_1 + \frac{L}{2} \left(1 - \cos \left(\frac{i-1}{P-1} \pi \right) \right), \quad i = 1, \dots, P \quad (22)$$

In the ζ - direction

$$\zeta_i = \frac{h_{sh}}{2} \left(1 - \cos \left(\frac{i-1}{N-1} \pi \right) \right), \quad i = 1, \dots, N \quad (23)$$

In this study, the following material properties are assumed for the conical shell

$$\begin{aligned} E_0 = 200 \text{ GPa}, \quad \nu = 0.3, \quad H_{0\zeta} = 5 \times 10^8 \text{ A/m}, \quad P_0 = 150 \text{ MPa}, \\ \alpha_0 = 1.2 \times 10^{-6} \text{ 1/}^\circ\text{C}, \quad \mu_0 = 4\pi \times 10^{-7} \text{ /m}, \quad K_0 = 181 \text{ /}^\circ\text{C} \end{aligned} \quad (24)$$

The results are expressed in terms of dimensionless characteristic quantities using the following non-dimensional parameters

$$\begin{aligned} \bar{\zeta} = \frac{\zeta}{h_{sh}}, \quad \bar{w} = \frac{w}{\zeta}, \quad \bar{T} = \frac{T}{T_i}, \\ \bar{\sigma}_{\zeta\zeta} = \frac{\sigma_{\zeta\zeta}}{P_0}, \quad \bar{\sigma}_{\theta\theta} = \frac{\sigma_{\theta\theta}}{P_0}, \quad \bar{h} = \frac{h}{H_{0\zeta}} \end{aligned} \quad (25)$$

At first, a convergence analysis is carried out to examine the computational efficiency of the DQ method. Distribution of the non-dimensional displacement \bar{w} , through the thickness with different numbers of DQ points is plotted in Fig. 2. It is observed from this figure that as the number of discrete points increases, the computed results rapidly converge. It is however noticed that even for less number of grid points, results with acceptable accuracy are obtained indicating the computational efficiency of the method.

Next, results obtained by the present method are compared with those of the finite element method which are found to be in good agreement, as shown in Fig. 3. Finite element analysis of the shell is carried out using ANSYS suit of program. The conical shell is modeled and meshed with Solid 5 element. It has eight nodes with up to six degrees of freedom per node and has 3-D magnetic, thermal, electric, piezoelectric and structural field capabilities with limited coupling between them.

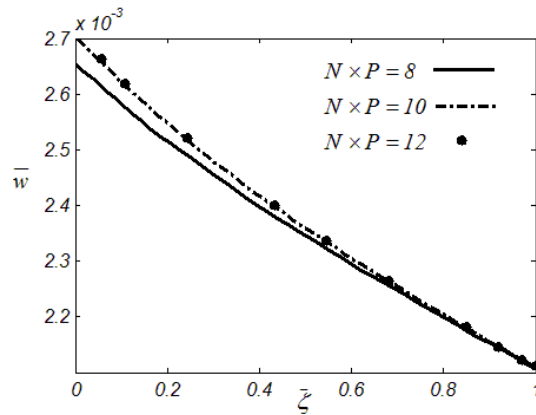


Fig. 2 Convergence study of DQ method, variation of \bar{w} with number of grid point

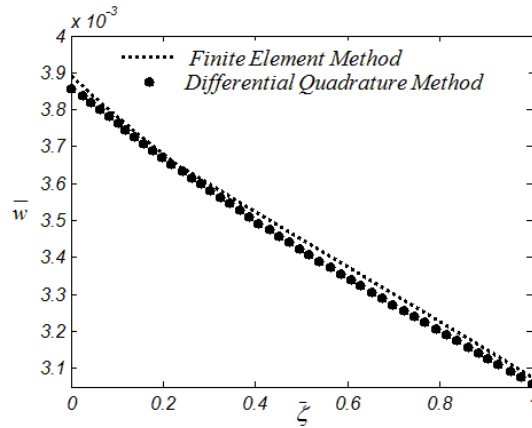


Fig. 3 Variation of \bar{w} with $\bar{\zeta}$, comparison of FEM with DQM

The effect of the power law index on the distribution of dimensionless components of displacement field \bar{w} , circumferential and radial stresses, induced magnetic vector and temperature fields through the thickness direction are shown in Figs. 4 to 8. It is depicted from Fig. 4 that the dimensionless displacement \bar{w} varies linearly across the thickness. It can be seen that as n changes from negative to positive the non-dimensional displacement decreases and for all cases the maximum and minimum values occur at the inner and outer surfaces, respectively. It is worth pointing out that for positive values of n the behavior of non-dimensional displacement is found to be fairly steady.

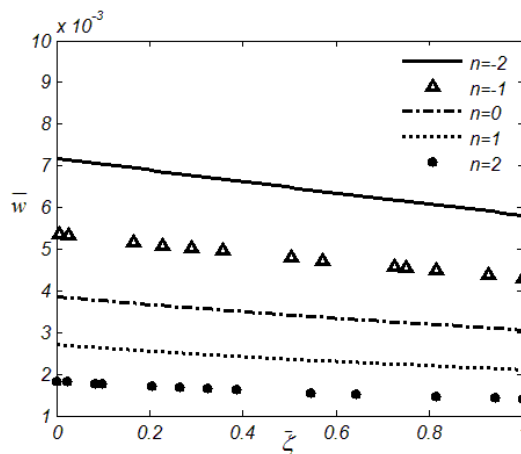


Fig. 4 Variation of \bar{w} with power law index of material properties

Variation of the stress component $\bar{\sigma}_{\zeta\zeta}$ with the value of power law index n , at different thickness points $\bar{\zeta}$ are shown in Fig. 5. It can be easily realized that the power law index has pronounced effect on the exerted stresses. As n changes from positive to negative, the distribution of the stress $\bar{\sigma}_{\zeta\zeta}$, along the thickness tends to decline. Consequently, one can choose appropriate FGM properties to reduce the value of induced stresses and promote the safety and structural integrity of functionally graded truncated conical shells.

The effect of power law index of material properties on distribution of the circumferential stress is depicted in Fig. 6. It is observed that the circumferential stress reaches its maximum value at the inner radius of the shell for negative values n and this trend is reversed for positive values of n . It is also observed that for $n = 0$, the circumferential stress remains almost steady and has nearly uniform distribution across the thickness. It is interesting to note that the value of this stress at $\bar{\zeta}$ approximately equal to 0.5 remains constant irrespective of the value of the grading index.

Distribution of the induced magnetic field of \bar{h} along the thickness for different values of the power law index is shown in Fig. 7. It is observed that as n varies from negative to positive, the absolute value of \bar{h} decreases. It is also noted that at $\bar{\zeta}$ approximately equal to 0.8, the value of the induced magnetic field remains constant for different values of power law index. Fig. 8 depicts distribution of temperature field along the thickness of the shell for different values of power law index. It is observed that as n changes from positive to negative value, the magnitude of the temperature at any position increases.

The effect of the thermal load on variations of dimensionless displacement \bar{w} , circumferential and radial stresses and induced magnetic vector fields through the thickness direction are shown in Figs. 9 to 12. The power law index is assumed to be equal to 1, i.e., $n = 1$. It is observed from Fig. 9, that as the temperature difference between the inner and outer surfaces increases, dimensionless value of the displacement component notably increases. Distribution along the thickness of $\bar{\sigma}_{\zeta\zeta}$ for different values of the inner-wall temperature is depicted in Fig. 10. It is observed from Fig. 10 that as the temperature difference across the wall of the shell increases the value of $\bar{\sigma}_{\zeta\zeta}$ slightly increases. These results can help designers to find an appropriate material property index for an FG truncated conical shell that contributes to lower values of thermal stresses.

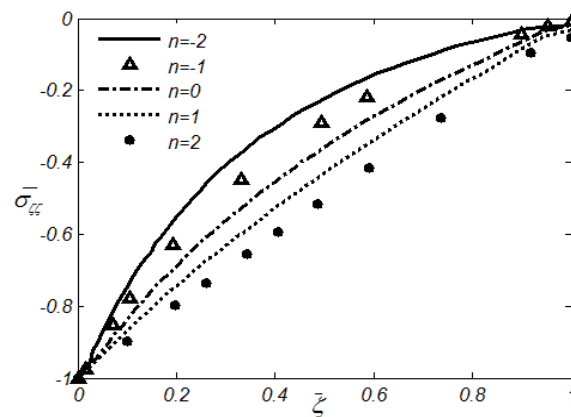


Fig. 5 Variation of $\bar{\sigma}_{\zeta\zeta}$ with power law index of material properties

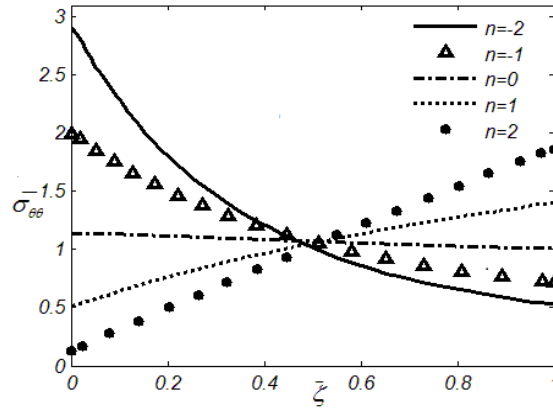


Fig. 6 Variation of $\bar{\sigma}_{\theta\theta}$ with power law index of material properties

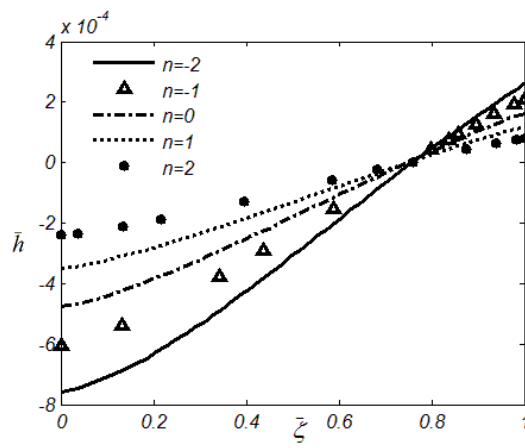


Fig. 7 Variation of \bar{h} with power law index of material properties

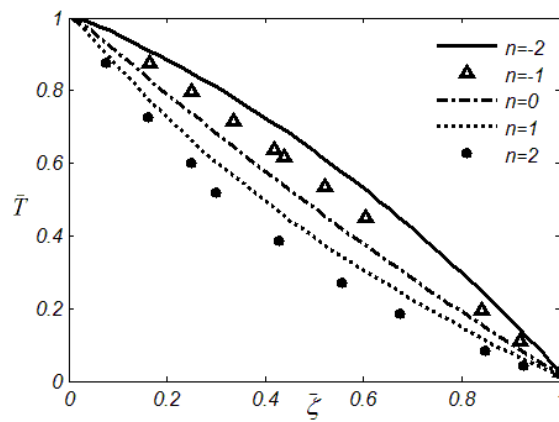


Fig. 8 Variation of \bar{H} with power law index of material properties

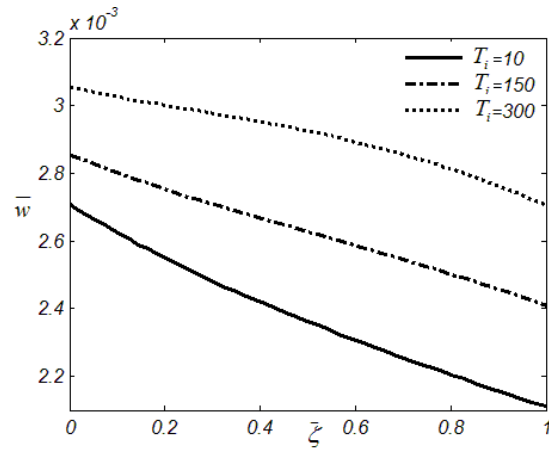


Fig. 9 Thermal load effect on variation of \bar{w}

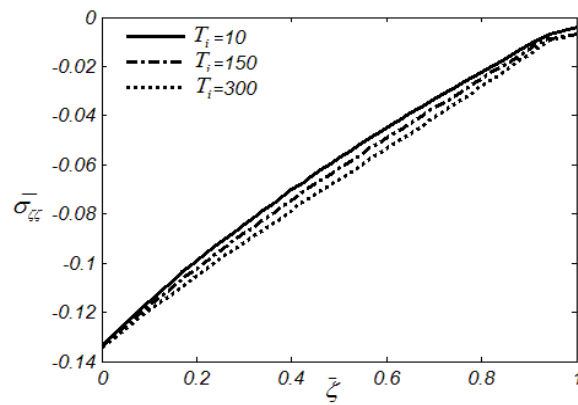


Fig. 10 Thermal load effect on variation of $\bar{\sigma}_{zz}$

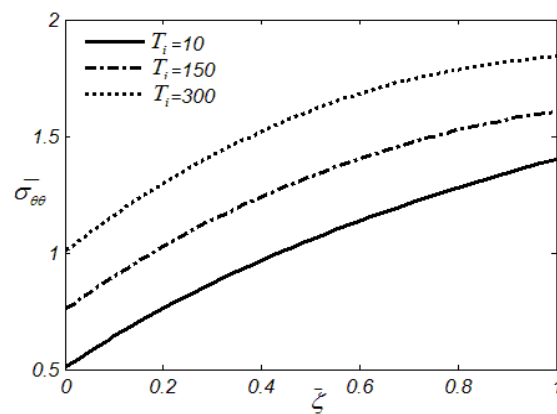


Fig. 11 Thermal load effect on variation of $\bar{\sigma}_{\theta\theta}$

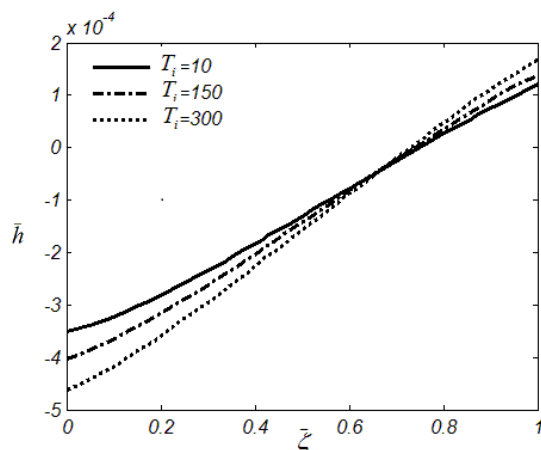


Fig. 12 Thermal load effect on variation of \bar{h}

Fig. 11 demonstrates the effect of the temperature gradient on the distribution of the dimensionless circumferential stress across the thickness of the truncated conical shell. As expected, value of circumferential stress considerably increases as the value of temperature difference across the shell increases. The maximum and minimum values of the non-dimensional circumferential stress in the FG conical shell always occur at its outer and inner surfaces, respectively. Variation of the induced magnetic field versus distance ζ in a conducting truncated circular conical shell for different values of temperature difference across the shell is shown in Fig. 12. It is noted that the maximum of absolute value of the induced magnetic field occurs at the inner surface and also approaches to zero for ζ about 0.7 irrespective to the value of temperature difference across the shell.

5. Conclusions

In this work, magneto-thermo-elastic analysis of a conducting truncated conical shell made of functionally graded material subjected to uniform magnetic and thermal fields and internal pressure is investigated. The constitutive formulas are derived and the differential quadrature method is employed to analyze the static magneto-thermo-elastic problem. It is concluded from above studies and results that the present solution is an accurate and effective technique and provides great numerical simulation. The numerical results are presented graphically and effects of power law index and thermal load on variation of the displacement, stress and thermal fields along the thickness are investigated. It is observed that magneto-thermo-elastic responses of the conducting non-homogeneous conical shell are mainly dependent on the non-homogeneity of material properties of the shell. The results introduced in the paper can assist engineers to select the desirable material property index to transcend the safety and structural reliability of an FG truncated conical shell.

References

- Aghdam, M.M., Shahmansouri, N. and Bigdeli, K. (2011), "Bending analysis of moderately thick functionally graded conical panels", *Compos. Struct.*, **93**(5), 1376-1384.
- Alibeigloo, A. and Nouri, V. (2010), "Static analysis of functionally graded cylindrical shell with piezoelectric layers using differential quadrature method", *Compos. Struct.*, **92**(8), 1775-1785.
- Chandrashekhara, K. and Kumar, B.S. (1993), "Static analysis of a thick laminated circular cylindrical shell subjected to axisymmetric load", *Compos. Struct.*, **23**(1), 1-9.
- Dai, H.L., Fu, Y.M. and Dong, Z.M. (2006), "Exact solutions for functionally graded pressure vessels in a uniform magnetic field", *Int. J. Solid. Struct.*, **43**(18-19), 5570-5580.
- Dai, H.L., Yang, L. and Zheng, H.Y. (2011), "Magnetothermoelastic analysis of functionally graded hollow spherical structures under thermal and mechanical loads", *Solid State Sci.*, **13**(2), 372-378.
- Eslami, M.R., Babaei, M.H. and Poultangari, R. (2005), "Thermal and mechanical stresses in a functionally graded thick sphere", *Int. J. Pres. Ves. Pip.*, **82**(7), 522-527.
- Ghannad, M., Zamani Nejad, M., Rahimi, G.H. and Sabouri, H. (2012), "Elastic analysis of pressurized thick truncated conical shells made of functionally graded materials", *Struct. Eng. Mech., Int. J.*, **43**(1), 105-126.
- John, K. (1941), *Electromagnetics*, McGraw-Hill Inc., New York, USA.
- Khdeir, A.A. (1996), "Thermoelastic analysis of cross-ply laminated circular cylindrical shells", *Int. J. Solids Struct.*, **33**(27), 4007-4017.
- Lee, Z.Y. (2009), "Magnetothermoelastic analysis of multilayered conical shells subjected to magnetic and vapor fields", *International Journal of Thermal Sciences*, **48**, 50-72
- Patel, B.P., Shukla, K.K. and Nath, Y. (2005), "Thermal postbuckling analysis of laminated composite cross-ply truncated circular conical shells", *Compos. Struct.*, **71**(1), 101-114.
- Shahani, A.R. and Nabavi, S.M. (2007), "Analytical solution of the quasi-static thermoelasticity problem in a pressurized thick-walled cylinder subjected to transient thermal loading", *Appl. Math. Model.*, **31**(9), 1807-1818.
- Shu, C. (2000), *Differential Quadrature and its Application in Engineering*, Springer-Verlag, London.
- Sobhani Aragh, B. and Yas, M.H. (2010), "Three-dimensional analysis of thermal stresses in four-parameter continuous grading fiber reinforced cylindrical panels", *Int. J. Mech. Sci.*, **52**(8), 1047-1063.
- Sofiyev, A.H. and Kuruoglu, N. (2011), "The non-linear buckling analysis of cross-ply laminated orthotropic truncated conical shells", *Compos. Struct.*, **93**(11), 3006-3012.
- Sofiyev, A.H. (2012), "The non-linear vibration of FGM truncated conical shells", *Compos. Struct.*, **94**(7), 2237-2245.
- Strang, G. (1986), *Introduction to Applied Mathematics*, Wellesley-Cambridge Press, Wellesley, MA, USA.
- Xing, Y. and Liu, B. (2010), "A differential quadrature analysis of dynamic and quasi-static magneto-thermo-elastic stresses in a conducting rectangular plate subjected to an arbitrary variation of magnetic field", *Int. J. Eng. Sci.*, **48**(12), 1944-1960.
- Ying, J. and Wang, H.M. (2010), "Axisymmetric thermoelastic analysis in a finite hollow cylinder due to nonuniform thermal shock", *Int. J. Pres. Ves. Pip.*, **87**(12), 714-720.
- Zhao, X. and Lie, K.M. (2011), "Free vibration analysis of functionally graded conical shell panels by a meshless method", *Compos. Struct.*, **93**(2), 694-664.
- Zielnica, J. (2012), "Buckling and stability of elastic-plastic sandwich conical shells", *Steel Compos. Struct.*, **13**(2), 157-169.

Nomenclature

K	Coefficient of heat conductivity
α	Coefficient of thermal expansion
σ_{ij}	Components of stress tensor
h_{sh}	Thickness of the shell
\vec{U}, u, w	Displacement vector and displacement components
L_1	Distance between the origin and the top surface of the cone
E_0	Elastic constant
\vec{J}	Electric current density vector
λ, G	Induced magnetic field vector
L	Lame's constants
f_l	Length of the generator of the cone
\vec{H}	Lorentz's force
μ	Magnetic field vector
N, P	Magnetic permeability
v	Number of grid points along the thickness and generator directions, respectively
n	Poisson's ratio
R_1, R_2	Power law index
γ	Inner radii of the cone at its small and large ends, respectively
$B^{(n)}$	Semi-vertex of the conical shell
$A^{(n)}$	Weighting coefficients of the n^{th} derivative along the generator